Metal Insulator Semiconductor Solar Cells Based on SiGe Virtual Substrates

Ziyad A. Altarawneh[*]

Electrical Engineering Department, Mutah University, Alkarak, Jordan
E-mail: zdtarawneh@mutah.edu.jo

Abstract— Recent research works on fabrication technologies of efficient solar cells indicate that fabrication cost is a major hurdle in adopting such devices in large-scale terrestrial applications. The cost reduction of solar cells can potentially emerge from technological advancements in the production of solar cells by utilizing multicrystalline or amorphous semiconductors rather than the conventional single crystal semiconductor solar cell. The characteristics of homojunction solar cells have been closely examined; however, such devices have high dark currents. Other alternatives are Metal Insulator Semiconductor (MIS) solar cells. The Si-MIS structures are very simple to fabricate and can possibly provide efficient solar cells. In this paper, a novel approach to improve the overall performance of the Si-based MIS solar cells by utilizing the SiGe layer as a virtual substrate is proposed. Extensive TCAD simulations are undertaken to investigate the overall electrical performance of the SiGe-based MIS solar cells. The simulation results show that the SiGe based devices outperform their Si counterparts. The electrical efficiency has reached up to 22.6%. Finally, the proposed MIS device is optimized in accordance with the findings of the key design parameters that influence the electrical efficiency of the cell such as the ratio of Ge in the SiGe substrate, thickness of the SiGe layer and thickness of the silicon layer.

Keywords— Metal insulator semiconductor; SiGe virtual substrate; Solar cells.

1.   INTRODUCTION

The necessity to secure an alternative clean energy resource has increasingly grown to be an international concern in recent years as a consequence of global climate warming and increased fuel prices. As a matter of fact, the annual global consumption of fossil fuels is predicted to be more than three-fourths of world energy use in 2040. Irrespective of the projected consistent rises in oil and gas prices, less than ten percent of the worldwide energy production in 2030 is anticipated to come from green energy sources, mostly hydroelectric, solar, wind, hydrothermal, and biomass [1]. In the recent years, a great deal of research efforts has been devoted to enhance the overall efficiency and reduce the manufacturing capacity of silicon photovoltaics. For instance, a novel surface texturing technique [2-4], antireflection coating engineering [5, 6], selective emitters in buried contact [7, 8], tunnel oxide passivated contacts [9, 10] and surface passivation methods [11] have been proposed to improve the optical and electrical performance of solar cells. Moreover, a transparent conductive oxide, such as indium tin oxide (ITO) nano-columns built into sub-wavelength surface structure on the solar cells, has also been employed for achieving good antireflection coating properties to improve their efficiency [12]. Possible cost reduction can potentially emerge from technological breakthroughs in the production of solar cells. One possible solution is Metal Insulator Semiconductor (MIS) solar cells. The Si-MIS structures are very simple to fabricate. However, in the past, they did not draw much attention due to their poor efficiency. Recently, Si-MIS structures are gaining more attention in photovoltaic cell

---

* Corresponding author

research studies. Both theoretical and experimental investigations indicate that the MIS technology could be considered as a possible low cost process for large area terrestrial solar cells while providing high open-circuit voltages (V_{OC}) [13-21]. Previously, the vast majorities of MIS solar cells are based on a single crystalline silicon, and have achieved efficiency from 15% to 18.5% [22]. Godfrey et al. reported that the achievable efficiency of such MIS solar cells are as high as 17.6%, approaching the best efficiency of their pn junction counterparts at that time which was 18.6% [23]. An efficiency of 17.1% was achieved when employing truncated pyramids at top and bottom layers of Si-MIS solar cells. However, this approach could increase the fabrication cost of solar cells [24]. Recently, Chang et al. has reported on a way to increase the V_{OC} using a stacking MIS solar cell structure [17], which integrates an n-type MIS solar cell with a p-type MIS solar cell. Moreover, MOSFET-like solar cells with voltage biasing is proposed in [25] with a maximum efficiency of 15.72% . More recently, the authors of [26] have proposed MOSFET solar cells with an antireflective transparent ITO in addition to plasmonic indium nano particles with the aid of an applied bias voltage. The obtained efficiency has reached up to 17.53%. Furthermore, Oener et al. have experimentally demonstrated nanowire based MIS solar cells with a measured efficiency of 7%, and an effective V_{OC} of 425 mV and estimated short-circuit current density (J_{SC}) of 23 mA/cm^2 [19]. In summary, these types of solar cells (i.e., MIS) have demonstrated some merits over conventional p-n junction solar cells, such as low cost fabrication process, simple structure, low temperature processing, and reasonably good efficiency.

One possible approach to improve the efficiency of the MIS solar cells is to adopt a low band-gap material in their structures. In this context, recent studies demonstrate that given their compatibility with the mature manufacturing process of the Si-based solar cells, the silicon germanium (SiGe) material is considered a promising candidate for improving and optimizing the solar cell optical and electrical performance. As a matter of fact, the photogeneration current in the small band-gap SiGe material is expected to offer a significant increase due to the improved absorption of photons in the near-infrared region of the solar spectrum. The V_{OC}, on the other hand, suffers from an inevitable drop due to the increase of the intrinsic carrier concentration associated with the decrease in the energy gap of SiGe [27]. Several studies have investigated the adoption of the SiGe materiel in various solar cell designs such as SiGe/Si hetero-junction solar cells and amorphous SiGe thin film solar cells. The authors of [28] have experimentally investigated the optimal Ge fraction in the SiGe layer of a hetero-structure thin film solar cell; and the overall efficiency of the solar cell was enhanced by about 4% more than that in the Si-based solar cell. The authors of [29] have numerically evaluated a single junction solar cell based on an a-Si:H/a-SiGe:H thin-film; and the achieved efficiency was 18.4%. Moreover, Hadi et al. have investigated the effect of Ge fraction on key performance parameters of SiGe based HIT solar cells. It was found that cell efficiency does not increase with higher Ge fraction due to the reduction in the band gap of the SiGe material [27]. More recently, Khan et al. have fabricated and characterized an epi-SiGe based heterojunctions solar cell with a low Ge fraction [30]. The cell efficiency was improved from 2.3% to 3.5%. In general, it is worth noting that the improved absorption behavior of the SiGe enhances the cell

photogeneration current; however, the induced reduction of the SiGe band gap negatively influences the cell's V_{OC}, which ultimately tends to undermine the benefits of adopting SiGe layer in the solar cell's structure. Therefore, finding the optimal structure for efficient SiGe based solar cells remains a significant challenge.

This paper presents a new MIS solar cell structure by utilizing a SiGe virtual substrate, extensive TCAD simulations and theoretical investigations on the electrical properties of the MIS based solar cells. Particular emphasis is placed on the optimal cell's structure that achieves the highest efficiency, which could enable its use in the mainstream solar cell industry. This paper is structured as follows. In Section 2, the structure, the doping profile, and the simulation setup for the proposed SiGe-based solar cell are presented. In Section 3, the calculated dependence of efficiency, J_{SC}, V_{OC} and fill factor (FF) of the proposed solar cell on key design parameters are presented and thoroughly discussed. In addition, an optimization process is performed in order to find the optimal structure of the proposed MIS solar cell. Finally, conclusions are drawn in Section 4.

2. THE PROPOSED SiGe-BASED MIS SOLAR CELL

Fig. 1 presents the cross-sectional view of the conventional Si-based MIS solar cell and the proposed SiGe-based MIS solar cell, respectively. In these structures, the top Aluminium monolayer acts as the metal electrode; the tunnelling oxide layer is very thin (typically < 15 A°); and p-type doped Si and SiGe layers act as absorption layers. The parameters of the SiGe, thin oxide and Si layers and doping density in each layer are presented in Table 1. For numerical simulations, 2D ATLAS simulator - a two-dimensional device simulation tool is used for modelling and investigating the electrical properties of the proposed MIS solar cell [31]. The cell's electrical equations such as Poisson, hole and electron continuity equations are used to evaluate the carriers' transport currents in the MIS structures [31]. The Shockley-Read-Hall and Auger models for Si and SiGe materials are used to estimate recombination currents. Moreover, LUMINOUS module is used to determine the photogeneration current in MIS solar cells by performing optical ray trace simulations in the cell's structure and determining the rate of light transmission and reflection [31]. The AM 1.5 radiation with incident power density of 100 mW/cm² is used as an illuminating source in this investigation. All TCAD simulations are undertaken at room temperature.
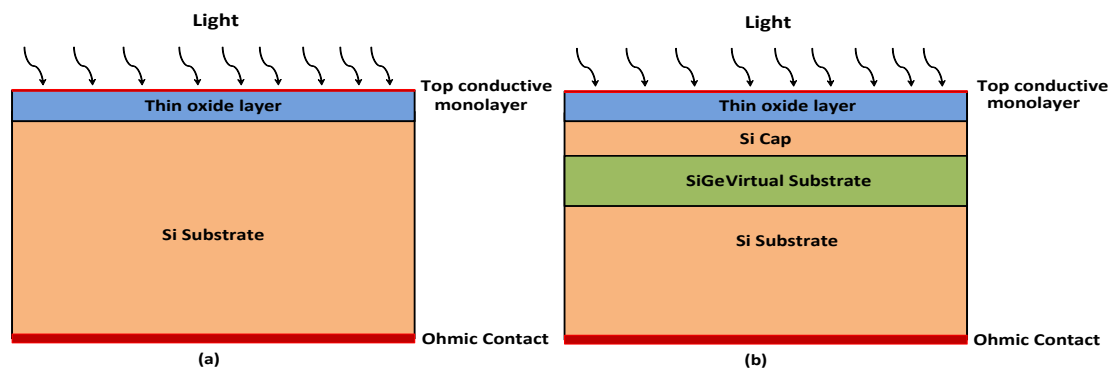

Fig. 1. Cross sectional view of: a) the conventional Si-based MIS solar cell; b) the proposed SiGe-based MIS solar cell.

Table 1. Design parameters of the proposed MIS solar cell's structure.

Parameter	Substrate doping [cm^{-3}]	Oxide thickness [A^o]	Si cap thickness [nm]	SiGe thickness [nm]	Cell thickness [μm]
Value	5×10^{17}	10	10	100	100

3.   RESULTS AND DISCUSSIONS

Figs. 3-6 illustrate the dependence of the obtained efficiency (E_{ff}), J_{SC}, V_{OC}, and FF on the absorber doping concentration (N_A) of both the conventional Si-based and the proposed SiGe-based MIS solar cell. The cell E_{ff} of the proposed solar cell is much higher than that of its conventional counterpart. The optimum substrate doping that achieves the maximum cell E_{ff} of the proposed solar cell is approximately 5×10^{17} cm^{-3}. The increase in the cell E_{ff} of the proposed MIS cell, as defined in Eq. (1), is primarily due to the improved light absorption which results from introducing the SiGe virtual substrate and enhancing the electrical mobility of both electron and holes in the SiGe layer. Consequently, this substantially increases the photo generation current and hence the J_{SC} of the proposed SiGe-based MIS solar cell as depicted in Fig. 4.

$$E_{ff} = \frac{P_{\max}}{P_{in}} = \frac{V_{oc}.J_{sc}.FF}{P_{in}} \tag{1}$$

where P_{max} is the maximum output power; and P_{in} is the incident solar power density.

Furthermore, the presence of a purposefully introduced SiGe layer between the Si substrate and the thin Si cap acts as a hole-blocking layer as shown in Fig. 2 from the energy band diagram of the proposed MIS solar cell. Hence, it reduces the recombination current at the front surface between oxide and Si-cap layers. Ultimately, it suppresses the dark current (J_{dark}) in the proposed solar cell, rendering an enhanced electrical performance.
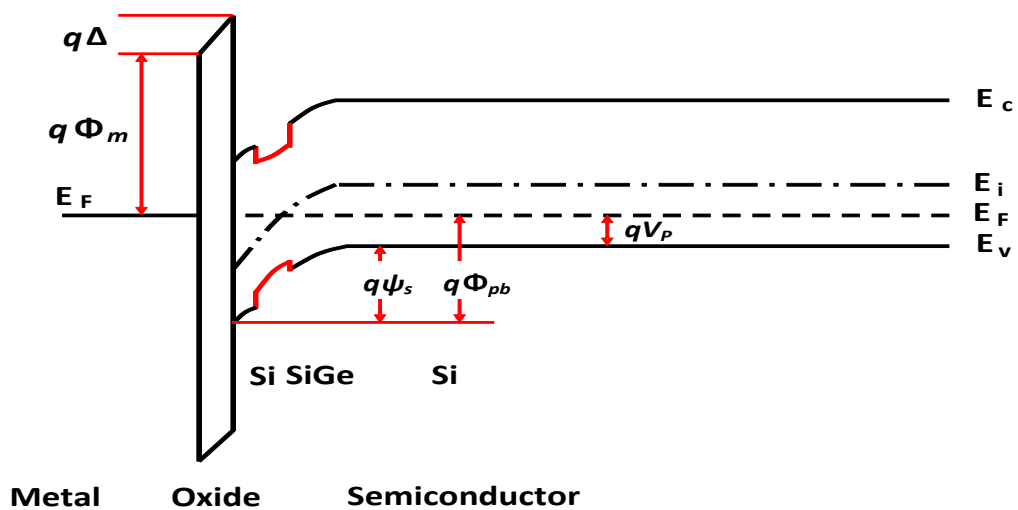

Fig. 2. Energy band diagram of the proposed SiGe-based MIS solar cell under equilibrium conditions.
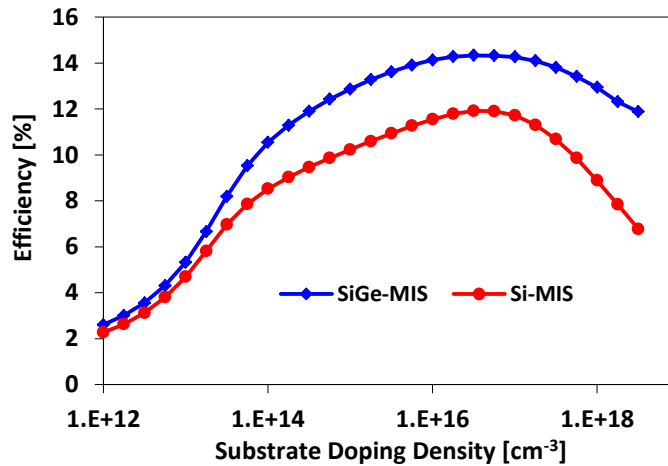
Fig. 3. Efficiency versus substrate doping density of the conventional and the proposed MIS solar cells.

For the J_{SC} shown in Fig. 4, it can be seen that as the doping density increases the J_{SC} increases until the doping density reaches a certain level (N_A= 2×10^{13} cm^{-3}). In this case, the front surface between Si and oxide layers starts to become thermally inverted until it reaches a strong inversion condition as the doping level increases. Therefore, J_{dark} is reduced due to the induced increase in the bending of conduction and valance bands (ψ_s) and the potential barrier height (Φ_{bp}) of the MIS solar cell as the doping level increases as evident from the Eqs. (2) and (3) [32].

$$\Phi_{bp} = \psi_s + V_p = \psi_s + \frac{kT}{q}\ln(\frac{N_V}{N_A}) \tag{2}$$

where N_V is the effective density of states in the valence band; T is the cell's temperature, and k is Boltzmann's constant. The potential barrier height is also related to the J_{dark} of the MIS cell by [32].

$$J_{Dark} = A**T^2 e^{(-\frac{q\Phi_{bp}}{kT})} e^{(-d_{ox}\cdot\sqrt{q\Phi_T})} \tag{3}$$

where $A**$ is the effective Richardson constant; $q\Phi_T$ is the average barrier height in the oxide layer; and d_{ox} is the oxide thickness.

This finally increases the J_{SC} density as the J_{dark} is reduced as given in the following equation [32]:

$$J_{SC} = J_{Light} - J_{Dark} \tag{4}$$

where J_{Light} is the total photogeneration current density.

For N_A higher than 2×10^{13} cm^{-3}, J_{SC} decreases. This is mainly because of the increased degradation in the diffusion length and lifetime of minority carriers while increasing substrate doping.

Considering the proposed MIS solar cell, it can be seen that E_{ff} and J_{SC} are significantly enhanced due to the presence of the SiGe layer in the cell's structure. This can be explained by the resulting increase J_{Light} induced under a steady illumination which can be given as the resultant current from the depletion and base regions in the cell's structure [33]:

$$J_{Light} = J_{Depletion} + J_{Base} \tag{5}$$

where $J_{Depletion}$ is the current density in the depletion region; and J_{Base} is the current density in the base region as given in the following equations:

$$J_{Depletion} = qT(\lambda)F(\lambda)(1 - e^{-\alpha w(\psi_s)}) \tag{6}$$

$$J_{Base} = qT(\lambda)F(\lambda)\left[\frac{\alpha L_{DL}}{\alpha L_{DL} + 1}\right]e^{-\alpha w(\psi_s)} \tag{7}$$

where $T(\lambda)$ is the transmission coefficient of the metal layer for the light of wavelength (λ); and $F(\lambda)$ is the number of incident photons/m²s per unit band width; and L_{DL} is the extrinsic Debye length of the hole under illumination conditions; and $w(\psi_s)$ is the width of the depletion region which is given in [13] as:

$$w(\psi_s) = \sqrt{\frac{2\varepsilon_s \psi_s}{qN_A}} \tag{8}$$

Furthermore, it can be seen from Fig. 2 that the SiGe layer is located in the depletion region where the electric field is extremely high so that the photo-generated carriers are swept out of the depletion region before they are combined towards the metallic contact. Therefore, as evident from Eqs. (5-8), the introduction of SiGe layer in the proposed cell structure increases J_{Light} due to the improved optical absorption coefficient of the SiGe material (a_{SiGe}) which is given as [34]:

$$\alpha_{SiGe} = \alpha_{Si}(1 - x) + \alpha_{Ge}(x) \tag{9}$$

where a_{Si} and a_{Ge} are optical absorption coefficients for the pure Si and Ge materials; and x is the Ge fraction in SiGe material.

Furthermore, V_{OC} increases the substrate doping density because of the decrease in the J_{dark} as demonstrated in the following Equation [32]:

$$V_{OC} = \frac{nkT}{q}\ln(\frac{J_{Light}}{J_{Dark}} + 1) \tag{10}$$

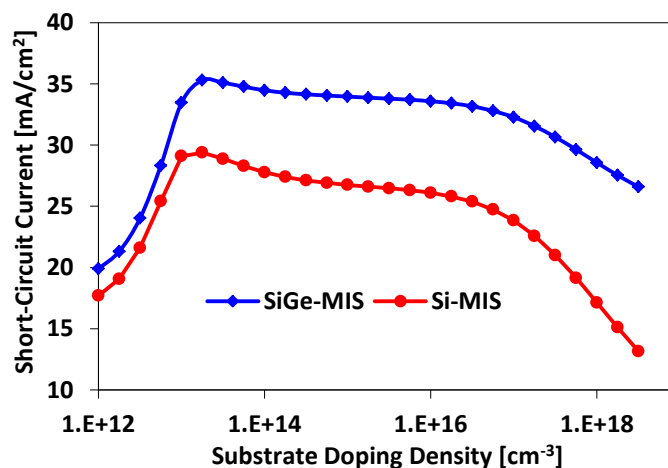where n is the ideality factor of the MIS p-n junction.

Fig. 4. Short-circuit current versus substrate doping of the conventional and the proposed MIS solar cells.

Furthermore, it can be seen from Fig. 5 that the introduction of the SiGe layer in the proposed MIS cell has a slight impact on its V_{OC} for low doping levels below

N_A= 5x10^{16} cm^{-3} compared with that of the conventional Si-based MIS solar cell. In this case, the value of J_{Light}/J_{Dark} is not affected by the presence of SiGe material as the induced enhancement in J_{Light} is almost cancelled out by the resulting increase in the J_{dark} in this layer. However, for N_A higher than 5x10^{16} cm^{-3}, the presence of the SiGe layer in the cell's structure reduces V_{OC}. This mainly results from the combined effect of the reduced lifetime of the carriers due to the increased doping levels and the induced reduction in the energy gap of SiGe layer which makes the recombination of carriers easier and further reduces the life time of carriers (τ_n) in SiGe layer leading to a higher J_{dark} (i.e leakage current). This can be represented J_{GR} as follows [13]:

$$J_{GR} = \frac{qn_i w(\psi_s)}{\tau_n}\left[e^{\left(\frac{q\Phi_s}{2kT}\right)} - 1\right]$$

(11)

where n_i is the intrinsic carrier concentration; and Φ_s is the difference between the electron and hole quasi-Fermi levels.
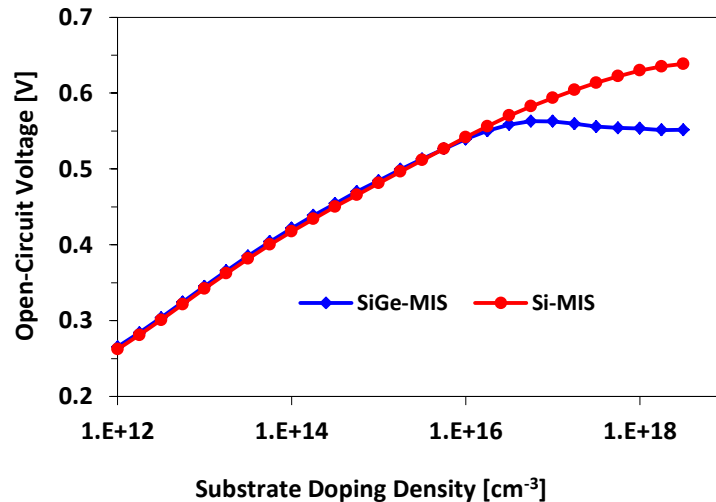

Fig. 5. Open–circuit voltage versus substrate doping of the conventional and the proposed MIS solar cells.

Moreover, as shown in Fig. 6, the *FF* initially decreases for low doping levels below N_A= 2x10^{13} cm^{-3} and then increases with increasing the doping level in the substrate until it reaches N_A= 1x10^{14} cm^{-3}. Thereafter, it slightly increases for higher doping levels. The behavior of FF of such solar cells depends on the behavior of their E_{ff}, J_{SC} and V_{OC}, as given in the following equation:

$$FF = \frac{P_{max}}{V_{OC} J_{sc}} = \frac{E_{ff} . P_{in}}{V_{OC} . J_{sc}}$$

(12)

Moreover, it can be seen that the FF of the proposed SiGe-based MIS solar cell is almost similar to that of its Si-based MIS counterpart due to the induced increase in J_{SC} and the reduction of V_{OC} when introducing the SiGe layer to the cell's structure.
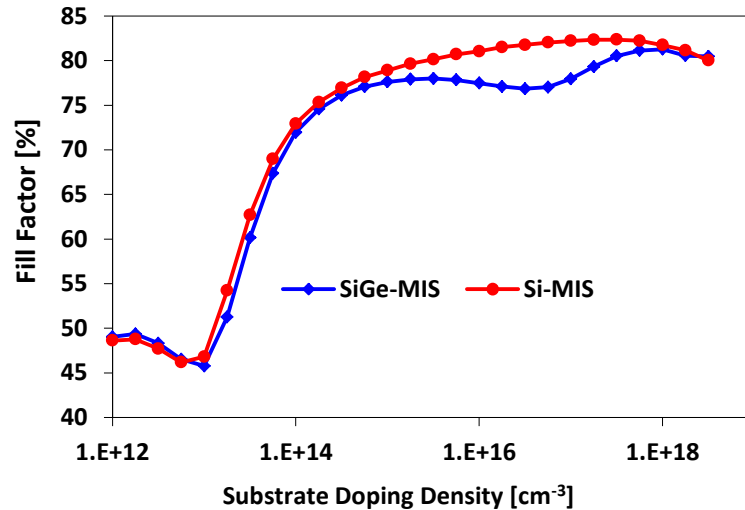
Fig. 6. Fill factor versus substrate doping of the conventional and the proposed MIS solar cells.

The d_{ox} is a critical parameter in the MIS cells, because it - in conjunction with other parameters - significantly affects the overall performance of MIS solar cells. Fig. 7 shows the influence of d_{ox} variations on the E_{ff} of the Si and SiGe based MIS solar cells. As the d_{ox} increases above a critical value of 15 A°, the solar cell current is limited by the rate at which carriers can tunnel between the metal and the semiconductor. As expected in this type of solar cells, the tunneling current decreases exponentially when increasing d_{ox} as shown in Fig. 8. In other words, a small current can tunnel through a thicker oxide leading to poor cell E_{ff}. In this case, the MIS solar cell can be considered similar to the conventional p-n junction solar cell with a large series resistance. For d_{ox} below 15 A°, E_{ff} rapidly increases with decreasing d_{ox} until it saturates to around 10% and 14.6% for the conventional Si-based and the proposed SiGe-based MIS solar cells, respectively. In this case, the tunneling of carriers occurs at a significant rate so that the opposing resistance of this process can be considered negligible. As such, all possible currents from the absorber are extracted. Variations can only occur when illumination density is changed, thus the E_{ff} saturates. In other words, the current flow has now semiconductor limitations [4]; and the cell can be thought of as a Schottky-diode. Considering the proposed MIS solar cell, it can be seen that the E_{ff} and J_{SC} are much higher than that of the conventional Si-based MIS solar cell. This improvement is mainly due to the significant increase in J_{Light} and the enhanced absorption of light spectrum as a result of introducing the SiGe layer in the cell's structure.

Fig. 9 also shows that the V_{OC} is almost constant when increasing d_{ox}, since it is very thin (tens of angstroms) as demonstrated in the following equation [33]:

$$V_{OC} = \frac{nkT}{q} \ln(\frac{J_{Light}}{A^{**}T^2} + \frac{q\Phi_{pb}}{kT} + \sqrt{q\Phi_T}\, d_{ox}) \tag{13}$$
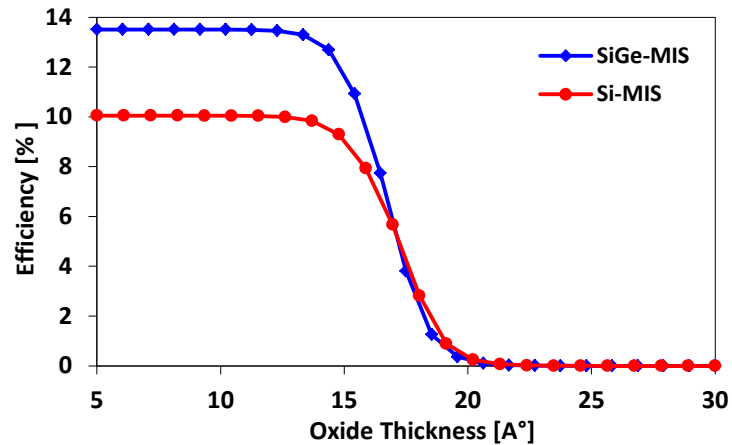
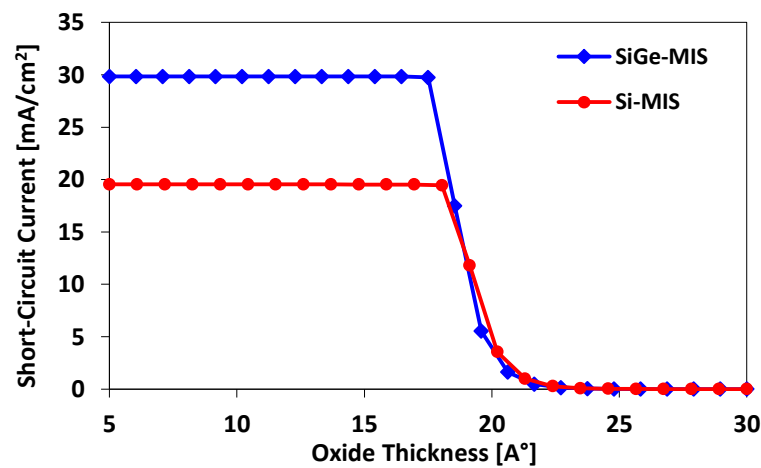Fig. 7. Efficiency versus oxide thickness of the conventional and the proposed MIS solar cells.

Fig. 8. Short-circuit current versus oxide thickness of the conventional and the proposed MIS solar cells.

In contrary to J_{SC}, V_{OC} of the proposed SiGe-based MIS solar cell is lower than that of the conventional Si-based MIS solar cell as shown in Fig. 9. This can be explained by the resulting increase in the J_{Dark} because of the induced reduction in the energy gap and lifetime of carriers in the SiGe layer.
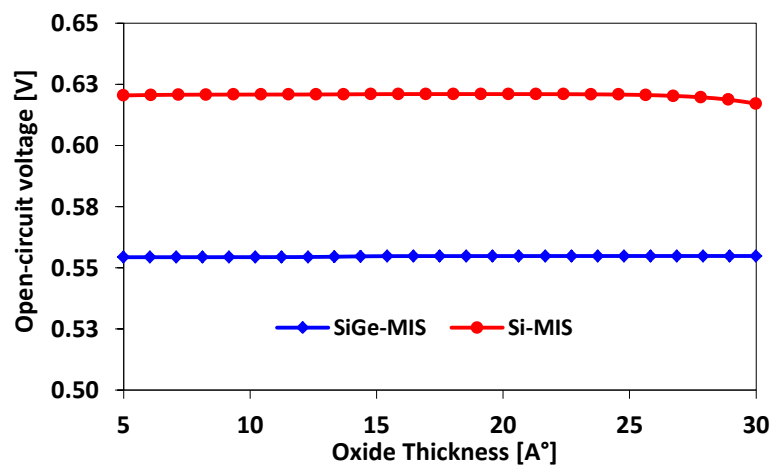

Fig. 9. Open–circuit voltage versus oxide thickness of the conventional and the proposed MIS solar cells.

Finally, the FF follows the behavior of J_{SC} and the cell's E_{ff} as shown in Fig. 10 since V_{OC} is almost constant. Moreover, the FF values of the proposed MIS solar cell are almost similar to those of the conventional Si-based solar cell. This is mainly due to the counterbalanced effect between the increased J_{SC} and the reduced V_{OC} of the proposed MIS cell as a result of introducing the SiGe layer to the cell's structure.
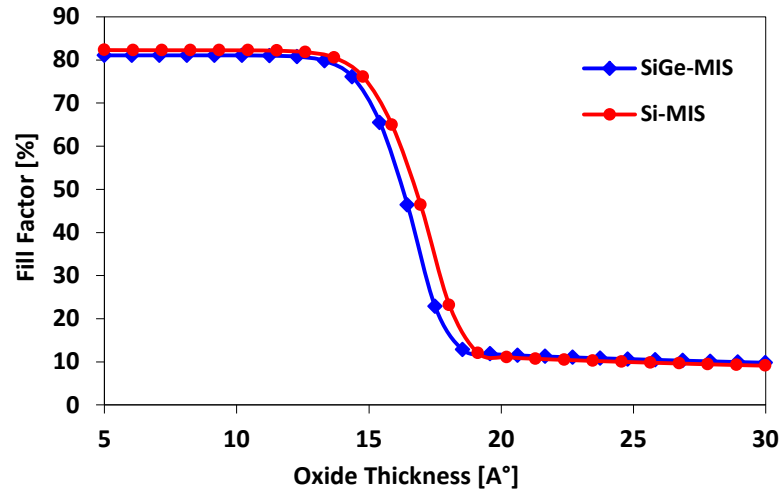

Fig. 10. Fill factor versus oxide thickness of the conventional and the proposed MIS solar cells.

Figs. 11-14 show the effect of choosing metals with different work functions (Φ_m) on the E_{ff}, the J_{SC}, the V_{OC} and the FF, respectively.

For metal work functions (Φ_m) less than 4.3 eV, the surface of Si interface is thermally inverted; and the effect of the J_{dark} can be considered negligible compared to J_{Light} ($J_{SC} \approx J_{Light}$) due to the increased band bending of conduction and valence bands as given in Eq. (14) [32]. Therefore, the variations in the J_{SC} and V_{OC} can only occur when illumination density is changed.

$$\psi_s = \Delta + \frac{E_g}{q} + \chi - \Phi_m - V_P \tag{14}$$

where Δ is the potential across oxide; E_g is the band gap of the semiconductor; χ is the electron affinity; and V_p is the Fermi level potential.

Fig. 12 reveals that J_{SC} remains constant for Φ_m between 4.3 eV and 4.9 eV. In this case, the semiconductor surface is not strongly inverted; however, when the cell is illuminated, the photo-generated electrons create an optical inversion layer at the Si front surface and J_{SC} is dominated by the J_{Light}. On the other hand, V_{OC} decreases as Φ_m increases due to the resulting increase in the J_{dark} since the cell is not strongly inverted. Consequently, the FF and the cell E_{ff} decrease as Φ_m increases.

Furthermore, for Φ_m above 4.9 eV, the surface state of the semiconductor starts to change from weak inversion to depletion. Therefore, the J_{dark} becomes a dominant component due to the increased recombination of carriers. Consequently, this leads to a significant reduction in J_{SC}; and hence it further reduces V_{OC}, FF, and the cell's E_{ff}.
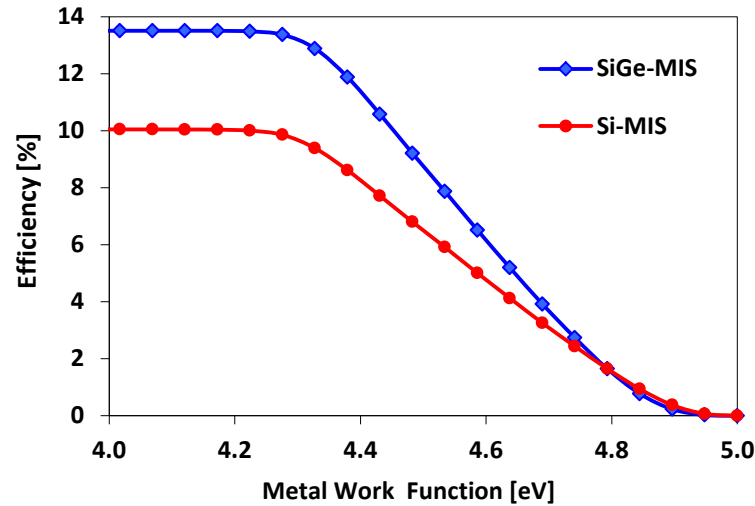
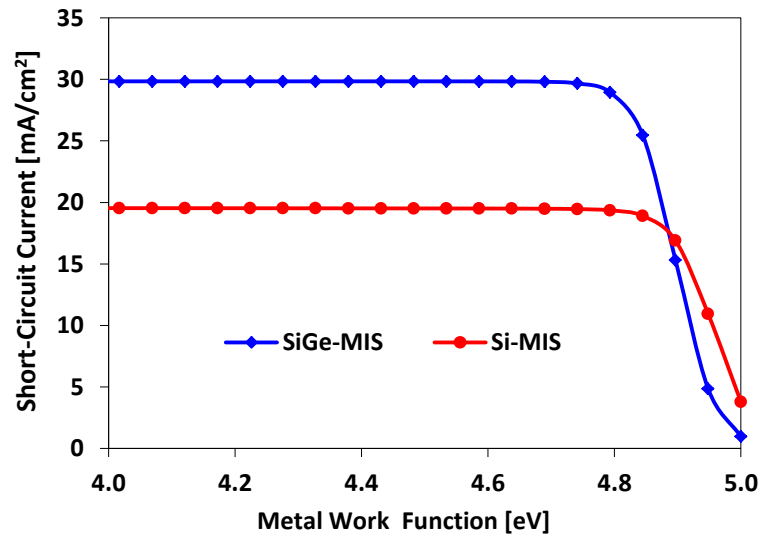Fig. 11. Efficiency versus metal work function of the conventional and the proposed MIS solar cells.

Fig. 12. Short-circuit current versus metal work function of the conventional and the proposed MIS solar cells.

Moreover, it can be seen that V_{OC} of Si-based MIS solar cells is much higher than that of SiGe-based MIS solar cells for Φ_m lower than 4.3 eV as shown in Fig. 13. The reduction of V_{OC} in the SiGe-based cell can be attributed to an induced increase in the J_{dark} due to the presence of the SiGe layer. However, for Φ_m above 4.3 eV, it can be seen that the values of V_{OC} of the proposed solar cell are almost similar to those of conventional solar cell. In this case, the SiGe-based cell is not strongly inverted; and the resulting increase in J_{Light} is undermined by the increased recombination current in SiGe layer.

Finally, it can be seen from Fig. 14 that the FF of the proposed solar cell is almost similar to that of conventional solar cell. However, for Φ_m = 4.3 - 4.9 eV, the FF of the proposed cell is significantly reduced due to the combined reduction in V_{OC} and J_{SC}.
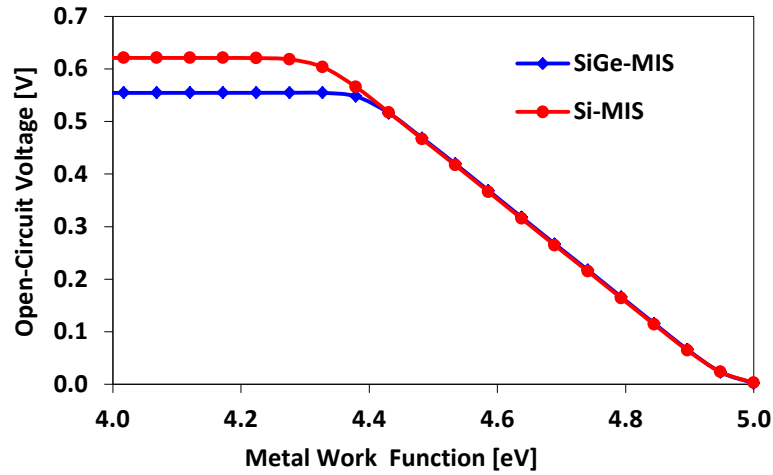
Fig. 13. Open-circuit voltage versus metal work function of the conventional and the proposed MIS solar cells.
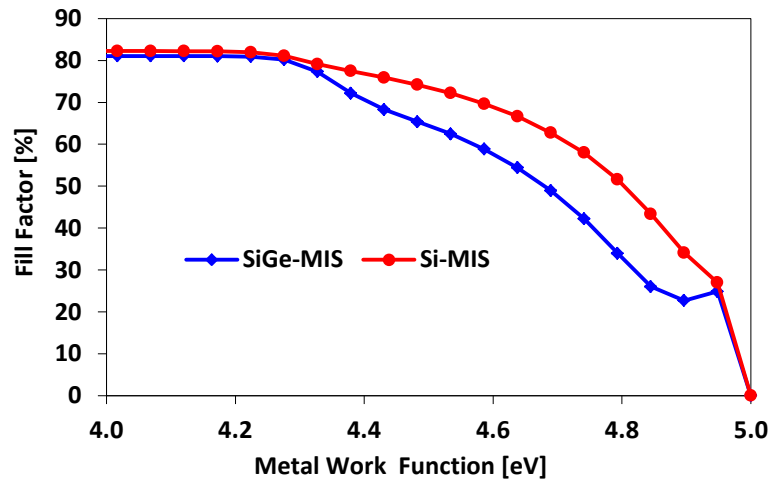

Fig. 14. Fill factor versus metal work function of the conventional and the proposed MIS solar cells.

Fig. 15 demonstrates the influence of the Ge fraction in the virtual SiGe substrate on the E_{ff} of the proposed SiGe-based MIS solar cell. The value of Ge fraction that can achieve the highest cell E_{ff} is almost equal to 0.5. The variation of Ge fraction modulates the energy gap of the SiGe material from Si (1.12 eV) to Ge (0.66 eV), which relates to absorbing a different band of the solar spectrum. The energy gap of SiGe material is calculated according to Vegard's law [34]:

$$E_{g\_SiGe} = (1 - x)E_{g\_Si} + xE_{g\_Ge} \tag{15}$$

where E_{g_Si} and E_{g_Ge} are the energy gaps for pure Si and Ge materials, respectively.

For Ge fraction (x) less than 0.5, the E_{ff} of the proposed MIS cell increases when increasing the Ge fraction in the SiGe substrate due to the improved absorption as the Ge fraction increases as evident from Eq. (9). However, for Ge fractions ($x = 0.5 - 0.67$), the cell's E_{ff} decreases when increasing x. This can be explained by the combined effect of the significant increase in the J_{dark} due to the carrier confinement phenomenon and the increased J_{Light}. For Ge fractions ($x = 0.67 - 0.91$), the induced increase in J_{Light} overcomes the increase in the J_{dark} due to the confinement effect. Consequently, the

cell's E_{ff} increases when increasing the Ge fraction. As the Ge fraction increases above ($x = 0.91$), J_{dark} starts to decrease again due to the increased reduction of the carrier's lifetime which yields a significant reduction in the E_{ff} of the proposed solar cell.
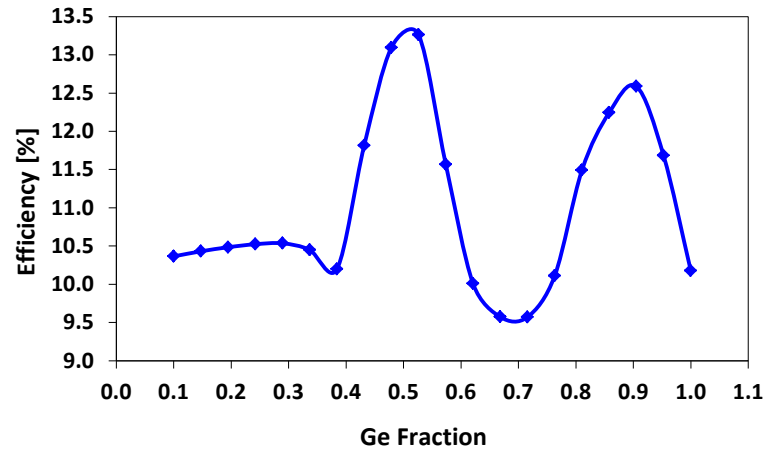

Fig. 15. Cell efficiency versus Ge fraction for the proposed SiGe-based MIS solar cell.

Fig. 16 shows that the J_{SC} increases as the Ge fraction increases to the value ($x = 0.5$) due to the improved absorption of the light at longer wavelengths. However, for Ge fractions $x = 0.5$ to 0.67, the photo-generated carriers start to be confined at the p-SiGe/p-Si heterointerface due to the induced offset in the valance band. Consequently, the recombination current is increased; and hence J_{SC} is reduced. For Ge fractions ($x = 0.67 - 0.91$), J_{SC} starts to increase until it reaches a maximum value of 34 mA/cm² for $x = 0.91$ due to the increased light absorption. After that, J_{SC} declines again due to the steep reduction in the energy band gap [35] and the associated increase in the recombination current which ultimately reduces J_{SC}.
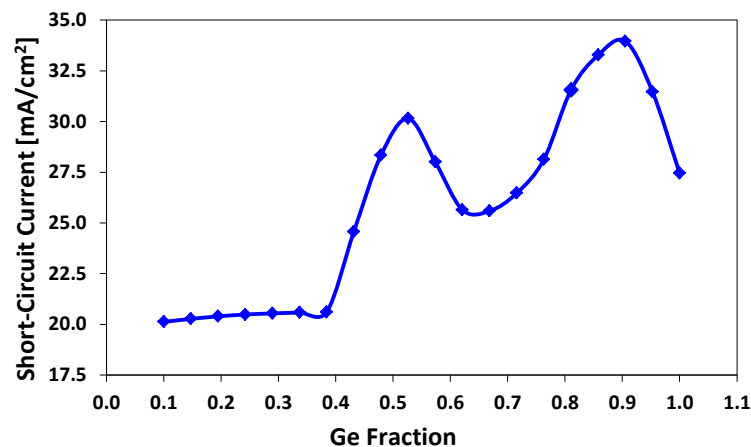

Fig. 16. Short-circuit current versus Ge fraction for proposed SiGe-based MIS solar cell.

Fig. 17 shows the effect of varying the Ge fraction in the virtual substrate on V_{OC} of the proposed MIS solar cell. For Ge fractions ($x = 0.1 - 0.4$), the ratio of J_{Light}/J_{Dark} remains almost constant due to the combined effect of the increased J_{Light}. The improved absorbance together with the increased J_{dark} results from the reduction in

energy band gap when increasing the Ge fraction in the SiGe layer. For Ge fractions (x= 0.4 - 0.8), J_{dark} starts to increase further due to the carrier confinement effect which ultimately dominates over the effect of the improved absorption in SiGe layer. Finally, for Ge fractions above 0.8, V_{OC} becomes almost constant since the increased J_{Light} is cancelled out by the increased J_{dark} due to the carrier confinement effect and the induced reduction in the band gap of the SiGe material.

Figure 18 demonstrates the influence of Ge fraction in the SiGe substrate on the FF of the proposed MIS solar cell. The FF follows the behavior of V_{OC} since the E_{ff} and J_{SC} of the proposed MIS cell have similar trends when increasing the Ge fraction in the virtual substrate as shown in Figs. 15 and 16.
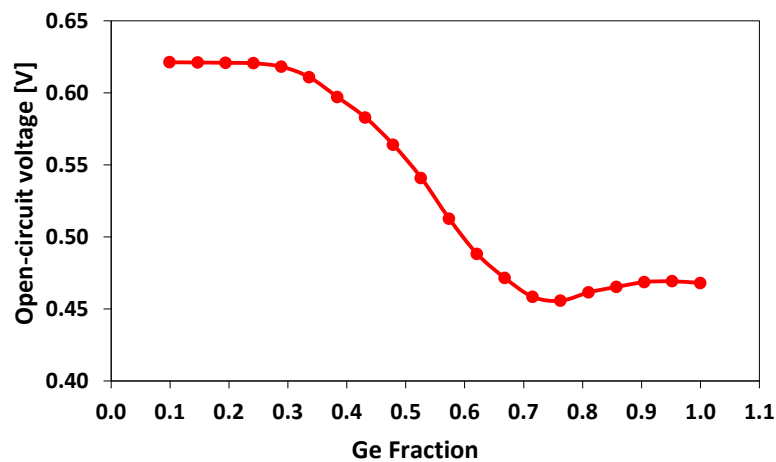

Fig. 17. Open-circuit voltage versus Ge fraction for the proposed SiGe-based MIS solar cell.
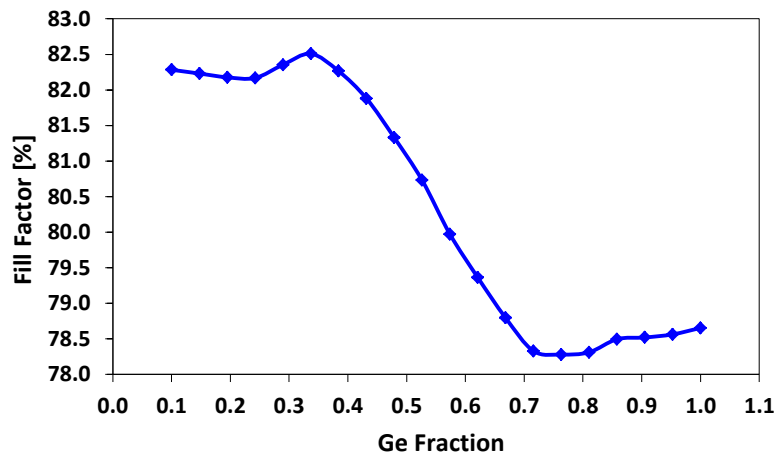

Fig. 18. Fill factor versus Ge fraction for the proposed SiGe-based MIS solar cell.

The silicon layer thickness plays an important role in the E_{ff} of the proposed MIS solar cell. It can be seen from Fig. 19 that adopting higher Si thickness reduces the cell's E_{ff}. As anticipated, the increase in the Si layer thickness reduces J_{SC} as shown in Fig. 20. This can be explained by the resulting decrease in the carrier generation rate, number of photons reaching the SiGe layer (absorber region), and the absorption coefficient of the Si layer as given in the following equation [13]:

$$G(\lambda, y) = \alpha(\lambda)T(\lambda)F(\lambda)e^{-\alpha y} \tag{16}$$

where the $G(\lambda,y)$ is the generation rate of the electron-hole pairs at distance y from the top surface.

The V_{OC}, on the other hand, is almost unaffected as the Si layer thickness increases due to the induced reduction in both J_{Light} and J_{dark} when increasing the thickness of the silicon layer. Finally, the FF of the proposed MIS cell follows the behavior of the E_{ff} and the J_{SC} when increasing the thickness of the silicon layer since the V_{OC} is almost constant.
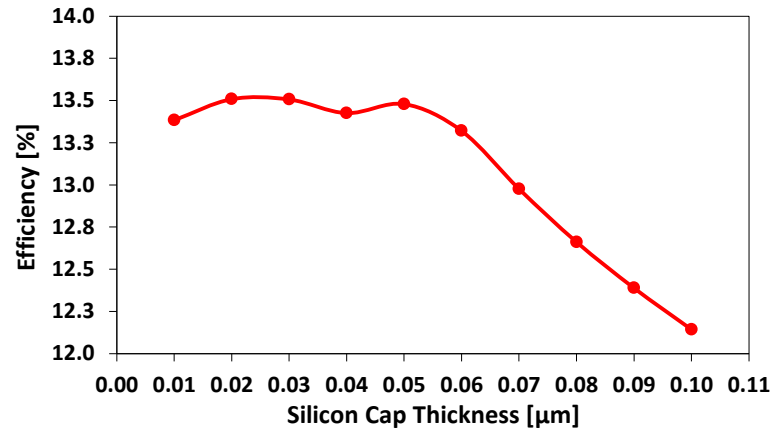
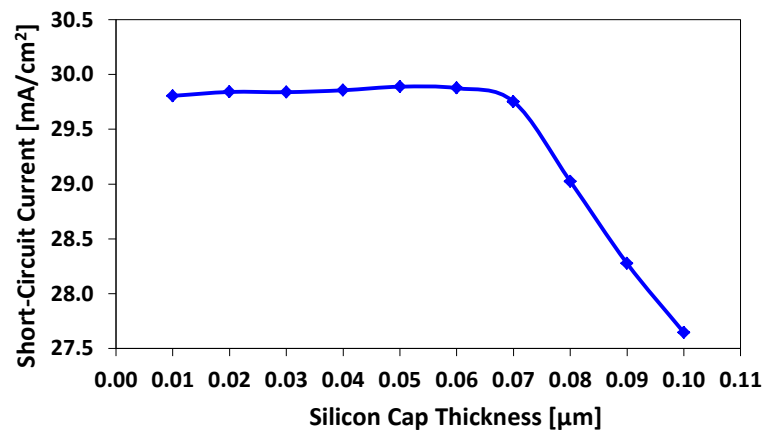Fig. 19. Efficiency versus silicon cap thickness of the proposed SiGe-based MIS solar cell.

Fig. 20. Short-circuit current versus silicon cap thickness of the proposed SiGe-based MIS solar cell.
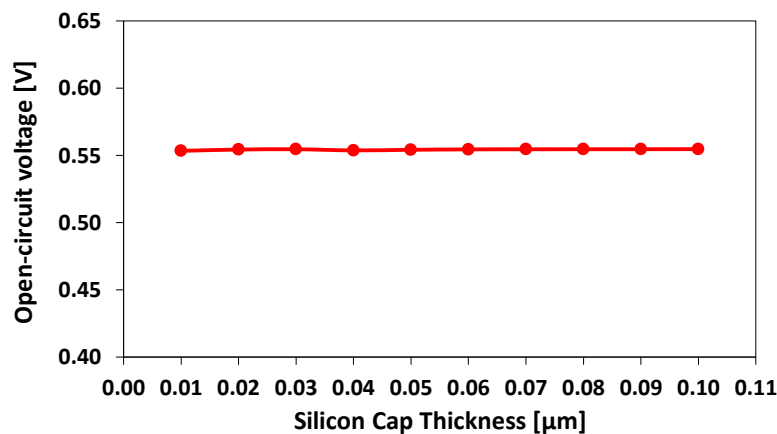
Fig. 21. Open-circuit voltage versus silicon cap thickness of the proposed MIS solar cell.
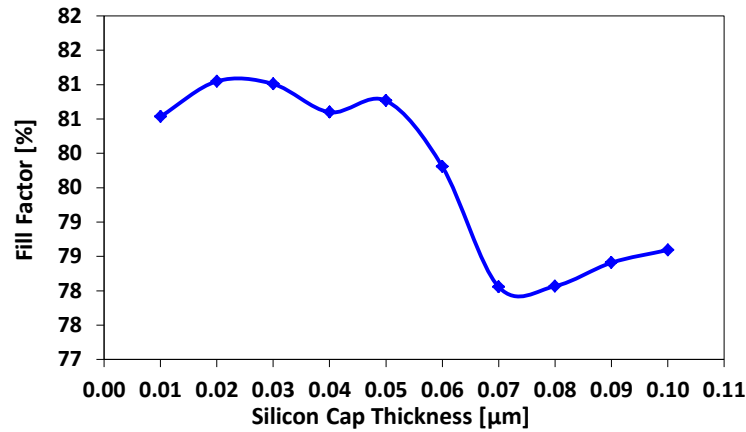
Fig. 22. Fill factor versus silicon cap thickness of the proposed SiGe-based MIS solar cell.

Fig. 23 shows the impact of the SiGe layer thickness on the E_{ff} of the proposed SiGe-based MIS solar cell. It can be seen that increasing the SiGe layer's thickness increases the E_{ff} due to the significant increase in J_{SC} as exhibited in Fig. 24. The cell's E_{ff} can reach up to 20%. It can be noticed that increasing the thickness of the SiGe layer increases the number of photo-generated carriers in the SiGe layer and the J_{Light} in the depletion and base regions, giving an enhanced cell performance. However, increasing the SiGe layer thickness reduces the V_{OC} as shown in Fig. 25. This is mainly due to the increased recombination current as the thickness of the SiGe layer increases.
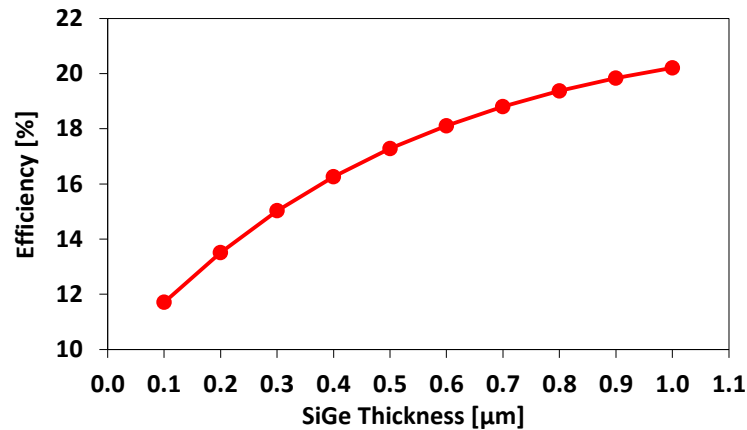

Fig. 23. Efficiency versus the SiGe layer thickness of the proposed SiGe-based MIS solar cell.
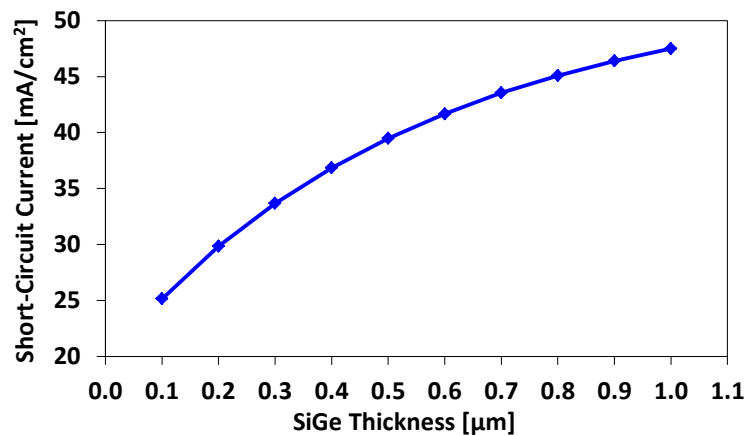

Fig. 24. Short-circuit current versus the SiGe layer thickness of the SiGe-based MIS solar cell.
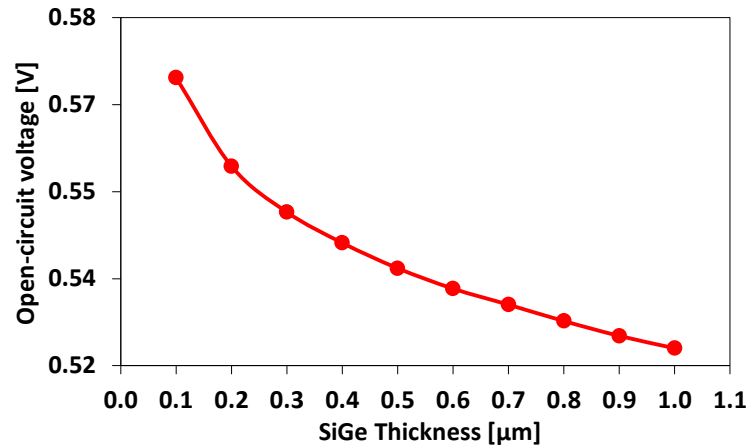
Fig. 25. Open-circuit voltage versus SiGe layer thickness of the proposed SiGe-based MIS solar cell.

A slight fluctuation in FF within the range of 80.7% and 81.1% is shown in Fig. 26. This can be attributed to the increase in J_{SC}, which is undermined by the decrease in the V_{OC} as the SiGe layer increases.
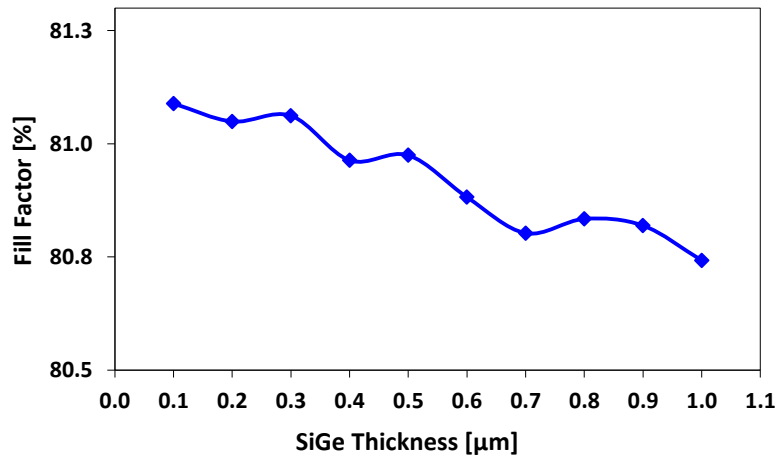
Fig. 26. Fill factor versus SiGe layer thickness of the proposed SiGe-based MIS solar cell.

Finally, an optimization process is undertaken to further improve the E_{ff} of the proposed SiGe-based MIS solar cell and find the optimal key design parameters that influence its overall performance. For this purpose, an automatic optimization process using Generic Algorithms (GA) is undertaken using the Virtual Wafer Fab (VWF) tool [36] to optimize the proposed cell's structure. The obtained results show that the E_{ff} of the optimal design could reach up to 22.6%. Tables 2 and 3 demonstrate the electrical performance of the optimal MIS solar cell and the associated key design parameters, respectively.

Table 2. Electrical performance of the optimal MIS solar cell.

E_{ff} [%]	J_{SC} [mA/cm²]	V_{OC} [mV]	FF [%]
22.6024	53.281	521.175	80.7932

Table 3. Key design parameters of the optimal SiGe-based MIS solar cell.

Substrate doping density [cm^{-3}]	Oxide thickness [A°]	Metal work function [eV]	Ge fraction	Si cap thickness [μm]	SiGe layer thickness [μm]
6.09x10^{+17}	6.98045	4.08242	0.42818	0.01112	5.75716

Table 4 shows the overall electrical performance of recently reported MIS solar cells. It can be seen that the proposed SiGe-based MIS solar cell has the highest conversion E_{ff} among recently reported MIS solar cells. The author of [17] has proposed a MIS based solar cell on a stacking structure of p and n layers. The reported E_{ff} was as low as 2.47%. In [24], an E_{ff} of 17.1% was achieved when employing truncated pyramids at top and bottom layers of a MIS solar cell. This approach, however, could increase the fabrication cost of solar cells. Moreover, a low-temperature anodization approach is utilized to fabricate the metal oxide semiconductor solar cell. The achieved E_{ff} in this work was 9.7% [15]. Furthermore, MOSFET like solar cells with a voltage biasing has been proposed in [25] where the reported E_{ff} ranges from 12.42% to 15.72% based on the applied biasing supply. More recently, MOSFET solar cells with antireflective transparent ITO and plasmonic indium nano particles under an applied bias were proposed in [26]. The maximum E_{ff} was 17.53%. Finally, the authors of [19] proposed nanowire network solar cells based on MIS technology. The experimental E_{ff} was 7.425%.

Table 4. Overall electrical performance of recently reported MIS solar cells.

Reference	E_{ff} [%]	V_{OC} [mV]	J_{SC} [mA/cm²]	FF [%]	Technology
[17]	2.47	0.71	5.49	58	MIS-Stacking Structure
[24]	17.1	639	35.5	75.5	MIS-truncated pyramids
[15]	9.7	415	33.4	70	MOS-anodization technique
[25]	12.42-15.72	540.8-559.4	29.51- 42.03	67-76	ITO/oxide/semiconduct or with voltage biasing
[26]	15.8-17.53 For In-NPs 16.87-17.80	553.4	45.76	70.6	MOS-antireflective/ITO and In NPs under applied bias voltage
[19]	7	425	23	58	MIS nanowire network
This work	22.6	521.175	53.281	80.7932	Based on SiGe virtual substrates

Moreover, when comparing the proposed MIS solar cell with other solar cell designs such as a Si heterojunction solar cell with interdigitated back contacts [37], it can be seen that the p-n junction based cells offer higher E_{ff}. However, the increased complexity in the cell's structure and the involved fabrication process's steps in addition to the increased thermal budget limit such solar cells from being adopted in

large-scale terrestrial applications. Therefore, the proposed SiGe-based MIS solar cell offers a possible solution for providing cheap solar cells with reasonably good electrical performance. Therefore, they can be taken into consideration for large scale terrestrial applications.

4. CONCLUSIONS

In this paper, a new SiGe-based MIS solar cell is proposed and its electrical performance is investigated through extensive TCAD simulations. In addition to that, the impact of the purposely-introduced SiGe region on the solar cell's performance is presented and thoroughly discussed. The simulation results show that the SiGe-based MIS solar cell outperforms its traditional Si-based MIS counterpart. Moreover, with appropriate design parameters such as the Ge fraction and the SiGe layer thickness, the conversion E_{ff} of the proposed cell can reach up to 22.6%. Therefore, the proposed cell's design has an excellent electrical performance, which makes it an appropriate candidate for large scale terrestrial applications.

REFERENCES

[1] International energy agency, "Energy efficiency outlook," *World Energy Outlook*, pp. 283-312, 2016.

[2] C. Chen, P. Juan, M. Liao, J. Tsai, H. Hwang, "The effect of surface treatment on omni-directional efficiency of the silicon solar cells with micro-spherical texture/ITO stacks," *Solar Energy Materials and Solar Cells*, vol. 95, no. 8, pp. 2545-2548, 2011.

[3] K. Chen, J. Zha, F. Hu, X. Ye, S. Zou, V. Vähänissi, J. Pearce, H. Savin, X. Su, "MACE nano-texture process applicable for both single- and multi-crystalline diamond-wire sawn Si solar cells," *Solar Energy Materials and Solar Cells*, vol. 191, pp. 1-8, 2019.

[4] J. Sheng, W. Wang, Q. Ye, J. Ding, N. Yuan, C. Zhang, "MACE texture optimization for mass production of high-efficiency multi-crystalline cell and module," *IEEE Journal of Photovoltaics*, vol. 9, no. 3, pp. 918-925, 2019.

[5] M. Chhajed, J. Kim, E. Schubert, "Nanostructured multilayer graded-index antireflection coating for Si solar cells with broadband and omnidirectional characteristics," *Applied Physics Letters*, vol. 93, no. 25, pp. 251108, 2008.

[6] X. Sun, X. Xu, J. Tu, P. Yan, G. Song, L. Zhang, W. Zhang, "Research status of antireflection film based on TiO2," *IOP Conference Series: Materials Science and Engineering*, vol. 490, pp. 1-6, 2019.

[7] J. Woehl, F. Granek, D. Biro, "19.7% efficient all-screen-printed back-contact back-junction silicon solar cell with aluminum-alloyed emitter," *IEEE Electron Device Letters*, vol. 32, no. 3, pp. 345-347, 2011.

[8] P. Procel, P. Löper, F. Crupi, C. Ballif, A. Ingenito, "Numerical simulations of hole carrier selective contacts in p-type c-Si solar cells," *Solar Energy Materials and Solar Cells*, vol. 200, pp. 1-7, 2019.

[9] S. Mitra, H. Ghosh, H. Saha, K. Ghosh, "Recombination analysis of tunnel oxide passivated contact solar cells," *IEEE Transactions on Electron Devices*, vol. 66, no. 3, pp. 1368-1376, 2019.

[10] A. Ingenito, G. Nogay, J. Stuckelberger, P. Wyss, L. Gnocchi, C. Allebé, J. Horzel, M. Despeisse, F. Haug, P. Löper, C. Ballif, "Phosphorous-doped silicon carbide as front-side full-area passivating contact for double-side contacted c-Si solar cells," *IEEE Journal of Photovoltaics*, vol. 9, no. 2, pp. 346-354, 2019.

[11] Y. Zhuang, S. Zhong, X. Liang, H. Kang, Z. Li, W. Shen, "Application of SiO_2 passivation technique in mass production of silicon solar cells," *Solar Energy Materials and Solar Cells*, vol. 193, pp. 379-386, 2019.

[12] C. Chang, P. Yu, C. Yang, "Broadband and omnidirectional antireflection from conductive indium-tin-oxide nanocolumns prepared by glancing-angle deposition with nitrogen," *Applied Physics Letters*, vol. 94, no. 5, pp. 051114, 2009.

[13] M. Doghish, F. Ho, "A comprehensive analytical model for metal-insulator-semiconductor devices: a solar cell application," *IEEE Transactions on Electron Devices*, vol. 40, no. 8, pp. 1446-1454, 1993.

[14] K. Lee, J. Hwo, "17.3% efficiency metal-oxide-semiconductor (MOS) solar cells with liquid-phase-deposited silicon dioxide," *IEEE Electron Device Letters*, vol. 18, no. 11, pp. 565-567, 1997.

[15] C. Wang, J. Hwu, "Metal oxide semiconductor structure solar cell prepared by low-temperature (<400°C) anodization technique," *Journal of The Electrochemical Society*, vol. 156, no. 3, pp. H181-H183, 2009.

[16] T. Chang, C. Chang, H. Lee, P. Lee, "Characteristics of MIS solar cells using sputtering SiO2 insulating layers," *35th IEEE Photovoltaic Specialists Conference*, pp. 001318-001321, 2010.

[17] T. Chang, C. Chang, H. Lee, P. Lee, "A metal-insulator-semiconductor solar cell with high open-circuit voltage using a stacking structure," *IEEE Electron Device Letters*, vol. 31, no. 12, pp. 1419-1421, 2010.

[18] Q. Lai, W. Ho, J. Liu, Y. Lee, C. Liao, J. Wu, Y. Chiu, "Photocurrent of MOS-Si photovoltaic device enhanced by an auxiliary biasing solar cell," *17th Opto-Electronics and Communications Conference*, pp. 701-702, 2012.

[19] S. Oener, J. van de Groep, B. Macco, P. Bronsveld, W. Kessels, A. Polman, E. Garnett, "Metal–insulator–semiconductor nanowire network solar cells," *Nano Letters*, vol. 16, no. 6, pp. 3689-3695, 2016.

[20] Z. Hafdi, "Amorphous silicon based MIS structures for solar cells applications: Electrical considerations," *1st International Conference & Exhibition on the Applications of Information Technology to Renewable Energy Processes and Systems*, pp. 20-25, 2013.

[21] M. Islam, M. Hasan, R. Sami, M. Chowdhury, "Modeling of graphene/SiO2/Si(n) based metal-insulator-semiconductor solar cells," *4th International Conference on the Development in the in Renewable Energy Technology*, pp. 1-4, 2016.

[22] R. Hezel, "Recent progress in MIS solar cells," *Progress in Photovoltaics: Research and Applications*, vol. 5, no. 2, pp. 109-120, 1997.

[23] R. Godfrey, M. Green, "655 mV open-circuit voltage, 17.6% efficient silicon MIS solar cells," *Applied Physics Letters*, vol. 34, no. 11, pp. 790-793, 1979.

[24] M. Grauvogl, A. Aberle, R. Hezel, "17.1% efficient truncated-pyramid inversion-layer silicon solar cells," *The Twenty Fifth IEEE Photovoltaic Specialists Conference*, pp. 433-436, 1996.

[25] W. Ho, M. Huang, Y. Lee, Z. Hou, C. Liao, "Performance enhancement of ITO/oxide/semiconductor MOS-structure silicon solar cells with voltage biasing," *Nanoscale Research Letters*, vol. 9, no. 1, pp. 1-5, 2014.

[26] W. Ho, R. Sue, J. Lin, H. Syu, C. Lin, "Optical and electrical performance of MOS-structure silicon solar cells with antireflective transparent ITO and plasmonic indium nanoparticles under applied bias voltage," *Materials*, vol. 9, no. 8, pp. 1-8, 2016.

[27] S. Abdul Hadi, P. Hashemi, N. DiLello, E. Polyzoeva, A. Nayfeh, J. Hoyt, "Thin-film $Si_{1-x}Ge_x$ HIT solar cells," *Solar Energy*, vol. 103, pp. 154-159, 2014.

[28] M. Liao, C. Chen, "The investigation of optimal Si-SiGe hetero-structure thin-film solar cell with theoretical calculation and quantitative analysis," *IEEE Transactions on Nanotechnology*, vol. 10, no. 4, pp. 770-773, 2011.

[29] A. Kosarian, P. Jelodarian, "Numerical evaluation and characterization of single junction solar cell based on thin-film a-Si:H/a-SiGe:H hetero-structure," *19th Iranian Conference on Electrical Engineering*, pp. 1-6, 2011.

[30] M. Ajmal Khan, R. Sato, K. Sawano, P. Sichanugrist, A. Lukianov, Y. Ishikawa, "Growth and characterization of low composition Ge_x in epi-Si_{1-x} Ge_x ($x \leq 10\%$) active layer for fabrication of hydrogenated bottom solar cell," *Journal of Physics D: Applied Physics*, vol. 51, no. 18, pp. 185107, 2018.

[31] Silvaco International, *Atlas User's Manual Device Simulation Software*, 2018.

[32] V. Yerokhov, I. Melnyk, A. Korovin, "External biasing as the factor of efficiency increase of silicon MIS/IL solar cells," *Solar Energy Materials and Solar Cells*, vol. 58, no. 2, pp. 225-236, 1999.

[33] R. Chauhan, P. Chakrabarti, "Influence of ionizing radiation on the performance of MIS solar cells: a theoretical model," *International Journal of Electronics*, vol. 89, no. 7, pp. 525-535, 2002.

[34] A. Singh, J. Tiwari, A. Yadav, R. Jha, "Analysis of Si/SiGe heterostructure solar cell," *Journal of Energy*, vol. 2014, pp. 1-7, 2014.

[35] Y. Shiraki, A. Sakai, "Fabrication technology of SiGe hetero-structures and their properties," *Surface Science Reports*, vol. 59, no. 7, pp. 153-207, 2005.

[36] Silvaco International, *Virtual Wafer Fab User's Manual*, 2018.

[37] M. Green, Y. Hishikawa, E. Dunlop, D. Levi, J. Hohl-Ebinger, A. Ho-Baillie, "Solar cell efficiency tables (version 51)," *Progress in Photovoltaics: Research and Applications*, vol. 26, no. 1, pp. 3-12, 2018.